Rainfall and Snowfall Observations by the Airborne Dual-Frequency Precipitation Radar During the Wakasa Bay Experiment

Simone Tanelli, Eastwood Im, Stephen L. Durden and Jonathan P. Meagher
Jet Propulsion Laboratory, California Institute of Technology
Pasadena, CA (USA)
simone.tanelli@jpl.nasa.gov

***Abstract*— Radar data obtained through the NASA/JPL Airborne Precipitation Radar APR-2 during the Wakasa Bay Experiment in January/February 2003 were processed to obtain calibrated reflectivity measurements, rainfall/snowfall velocity measurements, classification of the surface type and detection of the boundaries of the melting layer of precipitation. In this paper the processing approach is described together with an overview of the resulting data quality and known issues.**

Keywords-component; precipitation radar, field campaign

I. INTRODUCTION

Following the successful Precipitation Radar (PR) of the Tropical Rainfall Measuring Mission (TRMM) [1], a new airborne, 14/35 GHz rain profiling radar, known as Airborne Precipitation Radar – 2 (APR-2) [2], has been developed by NASA/JPL as a prototype for an advanced, dual-frequency spaceborne radar [3] for the TRMM follow-on mission – the Global Precipitation Mission (GPM). This airborne instrument is capable of making simultaneous measurements of rainfall parameters, including co-pol and cross-pol rain reflectivities and Doppler velocities, at 14 and 35 Ghz (*i.e.*, Ku and Ka band). Furthermore, it also features several advanced technologies for performance improvement, including real-time data processing, low-sidelobe dual-frequency pulse compression, and dual-frequency scanning antenna (24 beams uniformly distruibuted in the +/- 25 degrees cross-track range). The main radar parameters are shown in Table I.

APR-2 was operated on the NASA P-3 aircraft during the Wakasa Bay (Japan) experiment. The experiment conducted jointly by the U.S. AMSR-E and Japanese AMSR teams in Jan/Feb 2003, was designed to (i) validate both the AMSR and AMSR-E shallow rainfall and snowfall retrieval capabilities (ii) extend the database of rainfall properties needed to implement a comprehensive physical validation scheme, and (iii) extend our understanding of rainfall structures through the use of new remote sensing technology. On 12 flights, more than 30 hours worth of precipitation systems were observed, including rain and snow events, both over ocean and over land.

II. RADAR DESCRIPTION AND CALIBRATION

The APR-2 data quality has been assessed by examining a number of engineering parameters related to the radar's stability and calibration. Fig. 1 shows the observed minimum detectable reflectivity Z for APR-2 at both frequencies. This was derived from clear-air observations of the radar return signal and of the receiver noise floor (in Wakasa Bay experiment no pulse was transmitted in beam #1 of each scan in order to measure receiver noise). The values for both Ku-band and Ka-band are below 5 dBZ at 10 km range from the radar, however due to system non-linearities the effective minumum detectable reflectivity was approximately 5 dBZ already at 6 km range. The surface return, along with pulse compression sidelobes can be seen at approximately 6 km range.

TABLE I. APR-2 PARAMETERS

Airborne PR-2 Parameters		
Frequency	13.4 GHz	35.6 GHz
Polarization	HH,HV	HH,HV
Antenna diameter (effective)	0.4 m	0.14 m
Beamwidth	3.8 deg	4.8 deg
Antenna Gain	34 dBi	33 dBi
Antenna sidelobe level	-30 dB	-30 dB
Polarization Isolation	-25 dB	-25 dB
Peak Power	200 W	100 W
Bandwidth	4 MHz	4 MHz
Pulse Width	10-40 μs	10-40 μs
PRF	5 kHz	5kHz
6dB Pulse Width (after compression)	60 m	60 m
Range Bin Spacing	30 m	30 m
Horizontal res (a/c at 6 km alt)	400 m	500 m
Ground swath (a/c at 6 km alt)	4.5 km	4.5 km
Number of averaged pulses	250	250
Equiv. num. of independent samples	~60	~60
Noise equivalent Z_e (at 10 km range)	5 dBZ	5 dBZ
Doppler precision	0.4 m/s	>1 m/s

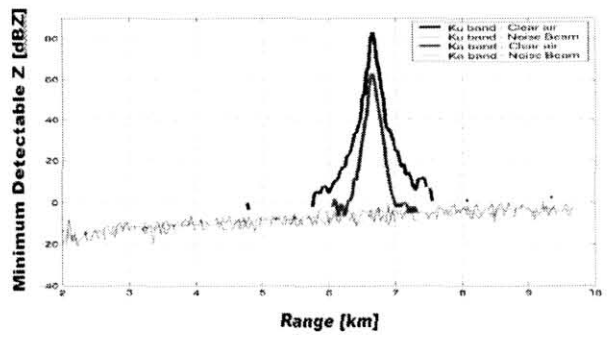

Figure 1. Observed minimum detectable reflectivity for APR-2 as a function of range. Surface return and pulse compression sidelobes are visible at around 6.7 km range.

Also of concern is the calibration of the radar. Calibration can be verified using observations of the ocean surface. This technique has been used previously with ARMAR [4], since the ocean backscatter near nadir is well known, especially near 10 degrees incidence, where sensitivity to wind speed is a minimum. Ocean backscatter at Ka-band is much less well characterized, although models show similar behavior to Ku-band. On the other hand, Ka band reflectivity in very light rain is expected to be nearly identical to that at Ku-band, since Rayleigh scattering should apply at both frequencies. In order to minimize the bias introduced by the different specific attenuation at the two frequencies, Ka-band calibration was verified relatively to Ku band by comparing returns in the top portion of very light rain areas (portions without a significant brightband between rain and radar were available within the dataset).

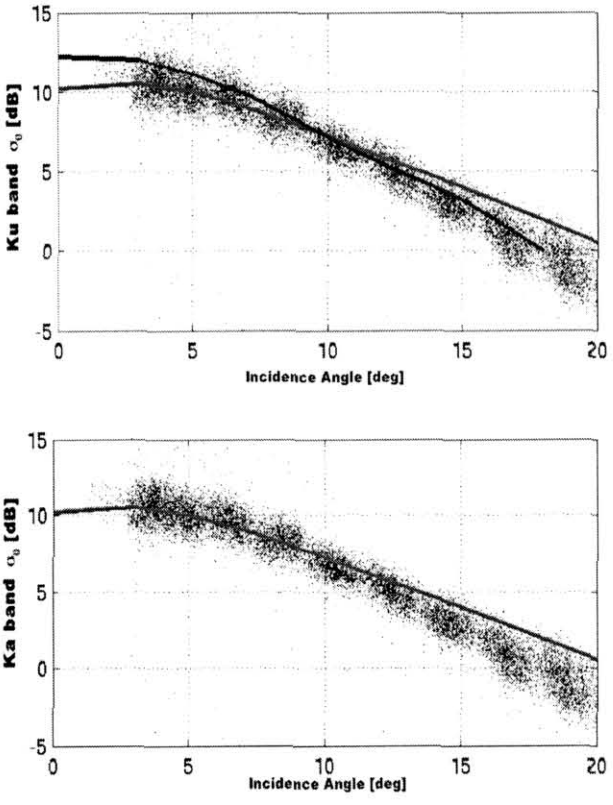

Figure 2. APR-2 observations of ocean backscatter versus incidence angle (4 different flights). Black: APR-2 measurements, Red: GMF, Blue: TRMM/PR global mean

Observations of the ocean surface with APR-2 show a Ku band normalized cross section of about 7.1 dB at 10 degrees incidence angle, which is close to previous measurements and models. Ocean backscatter observations from APR-2 in different wind conditions are shown in Fig 2. Comparison with surface reflectivities calculated with GMF or from TRMM/PR measurements seem to indicate small a bias of less ~0.5 dBZ, however strong winds and clouds undetected by APR-2 are possible contributors for this bias at Ku band, in depth analysis is required to further refine calibration. The Ka-band data have reflectivities within about 1 dB of the Ku-band reflectivities in light rain.

In the Wakasa Bay Experiment configuration the cross-polariztion leakage at Ka band was larger than nominal. It was estimated at –17.4 dB through observation of clear air, vertical incidence returns of ocean surface. By removing this leakage the useful range of LDR measurements at Ka band was reduced at about –15 dB. The cross-polarization leakage of the Ku band channel was at nominal values, hence LDR measurements at Ku band as low as –25 dB were obtained.

III. Correction for Aircraft Motion and Navigation Errors

Correct navigation is a critical aspect in producing correct and usable radar data. In particular, errors in estimating the aircraft motion, and/or the antenna angle relative to both the aircraft bearing and the earth surface result in errors in: a) correction for the aircraft motion contamination on Doppler velocity measurements, b) external calibration of the radar using the ocean surface backscattering, c) comparing/integrating with measurements obtained through other instruments. While the latter is significant only for relatively large errors (e.g., angle errors equivalent to one or more radar beamwidths), the former two are sensitive also to sub-beamwidth errors. As far as the specific configuration used for the Wakasa Bay experiment is concerned, errors in the navigation parameters occurred because of turbulence (the P-3 operates at relatively low altitude), lack of coregistration of radar data with navigation data (the latter being recorded only once per second), and uncertainty in the relative orientation of the radar reflector with respect to the aircraft reference system.

Navigation errors were corrected over ocean by minimizing two error functionals based on the comparison of two parameters of the radar apparent surface and the corresponding values calculated through the navigation parameters: the surface altitude and its Doppler velocity. Both functionals weigh more the measurements obtained at incidence angles smaller than 15 deg since the effects of range limitation and the resulting effects increase towards the margins of the scan.

The optimization procedure resulted in small residual errors both in roll angle (less than 0.2 deg in average) and apparent surface velocity (see Figure 3 for an example). A very small

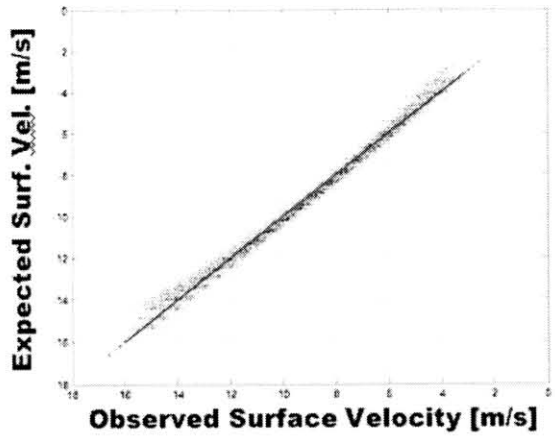

Figure 3. Comparison of observed and predicted Doppler from the ocean surface. The bias is 1 cm/s and the rms is 0.37 m/s.

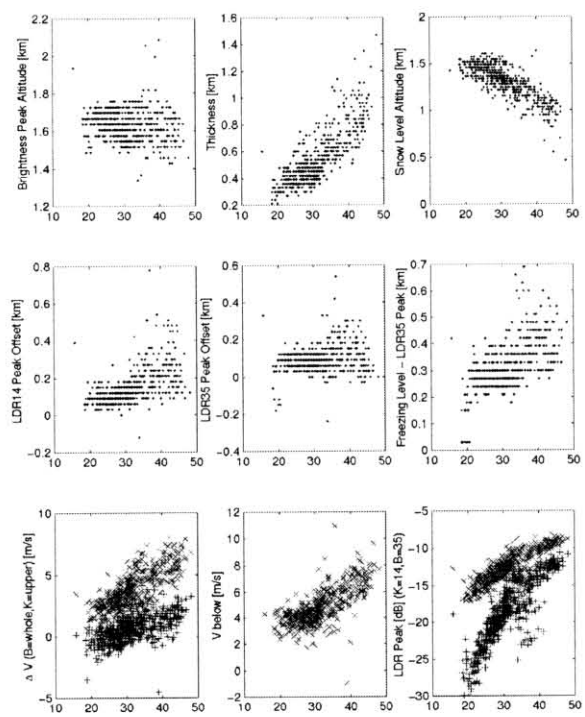

Figure 4. Parameters characterizing the melting layer of precipitation. The abscissa is the maximum brightband reflectivity (in dBZ) at Ku band for all scatterplots

number of scans still shows larger anomalies due to occasional, short-term (i.e., less than 1 second) movements of the aircraft due to turbulence, or aircraft maneuvers.

IV. Data Products

Three classification algorithms complete the software package for APR-2 data processing of: a Surface Classification algorithm (SC), a Bright Band Detection algorithm (BB) and a Precipitation Classification algorithm (PC). Each one was developed to make full use of the unique set of characteristics of APR-2: high resolution (30 m vertical, ~500 m horizontal), three-dimensionality, multipolarimetry, dual-frequency and Doppler capabilities. In particular, SC and BB are necessary for accurate calibration and correction of navigation errors and are therefore embedded in the preliminary radar processing steps.

The output of SC is a surface index unique for each radar scan that can assume 6 values. Two values indicate ocean surface (one for aircraft in level flight, and one for aircraft not in level flight), two indicate flat land (level flight/non level flight), 1 for rough terrain/hills, and one for antenna not scanning (no classification available for the surface). Examples of SC outputs are visible in Figures 5 and 6 (see figure caption for color key).

The output of the BB algorithm is a set of parameters characterizing the radar signature of the melting layer of precipitation: the upper and lower boundaries of the mixed phase region, the altituide at which each of the 5 APR-2 parameters reaches its maximum within the boundaries, the thickness of each signature and the altitude at which the Doppler velocity second derivative changes. An example of BB output is shown in Figure 4.

The output of PC is an index that can assume 6 values indicating: cloud, melting layer, stratiform precipitation, deep convection, snowfall, other. It relies on the output of the BB algorithm and on a three-dimensional morphological algorithm.

Conclusions

The NASA/JPL airborne precipitation radar APR-2 collected more than 30 hours of data during the Wakasa Bay Experiment in January and February 2003. The whole dataset was processed for external calibration, correction of navigation errors and contamination of Doppler measurements by aircraft motion. Three classification algorithms have been developed for APR-2 and provide excellent performances.

Acknwledgment

The research described in this paper was performed at the Jet Propulsion Laboratory, California Institute of Technology, for the AQUA/AMSR-E validation program under contract with the National Aeronautics and Space administration

References

[1] C. Kummerow et al., "The Tropical Rainfall Measuring Mission (TRMM) sensor package," *J. Atmos. Oceanic Technol,* vol. 15, pp. 809-817, 1998.

[2] G.A. Sadowy, Berkun, A.C., Chun, W., Im, E., Durden, S.L., "Development of an advanced airborne precipitation radar", *Microwave Journal,* vol 46, n 1, January, 2003, p 84-98.R. Nicole, "Title of paper with only first word capitalized," J. Name Stand. Abbrev., in press.

[3] E. Im et al., "Second-Generation Spaceborne Precipitation Radar, Proc. IGARSS 2000.

[4] S. L. Durden, E. Im, F. K. Li, W. Ricketts, A. Tanner, and W. Wilson, ``ARMAR: An airborne rain mapping radar," *J. Atmos. Oceanic Technol.*, vol. 11, no. 3, pp. 727-737, 1994.

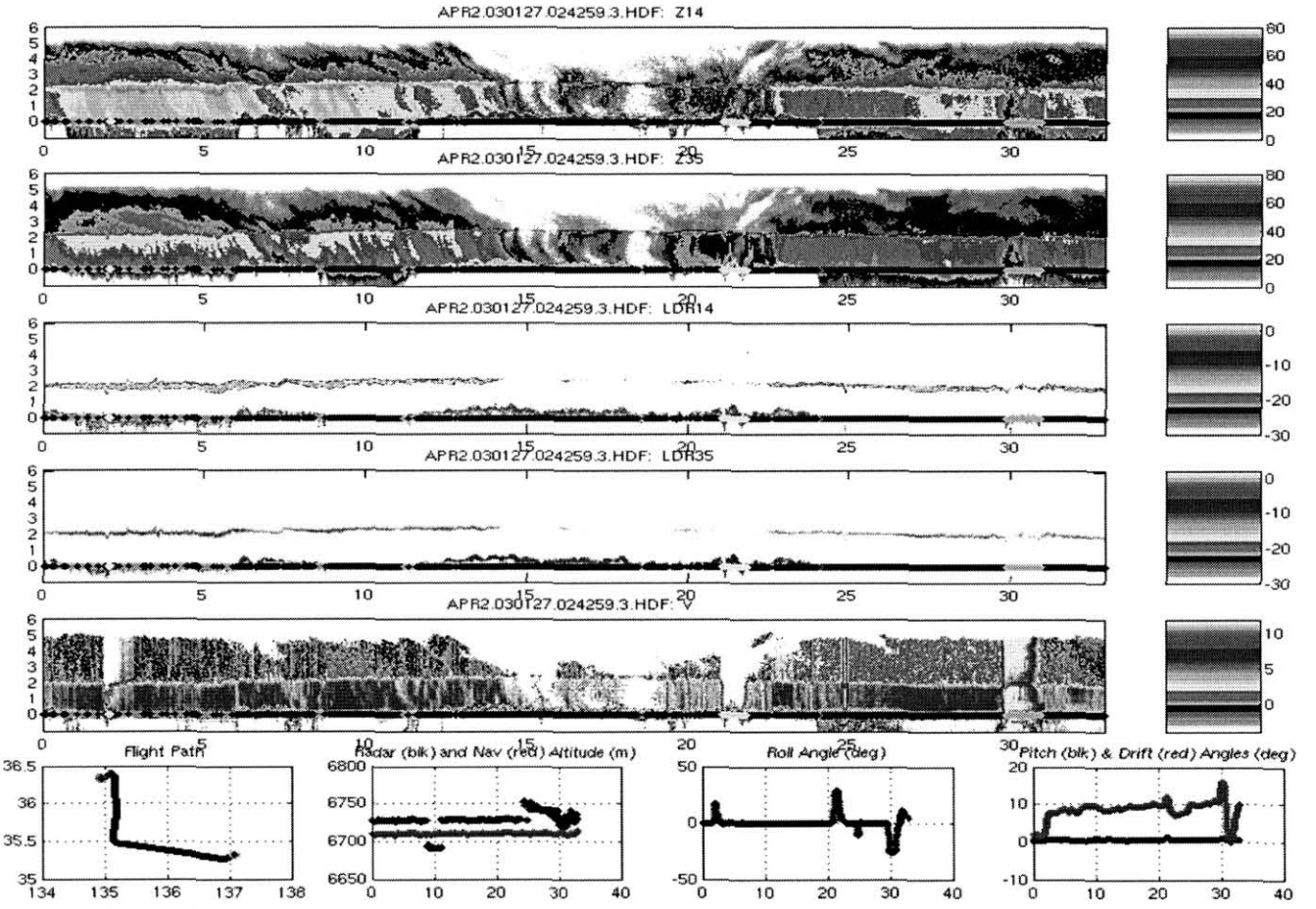

Figure 5. Stratiform precipitation over ocean and over land starting at 05:43 UTC on Jan. 19th 2003. Panels a – e: time of observation (in minutes) is shown in the horizontal axis and the altitude (in km a.s.l.) is on the vertical axis. The value of the surface index is shown at altitude 0: blue=ocean, cyan=ocean (a/c maneuvering), black=rough terrain/hill, green = flat land, yellow=flat land(a/c maneuvering). The four insets at the bottom show the navigation parameters.

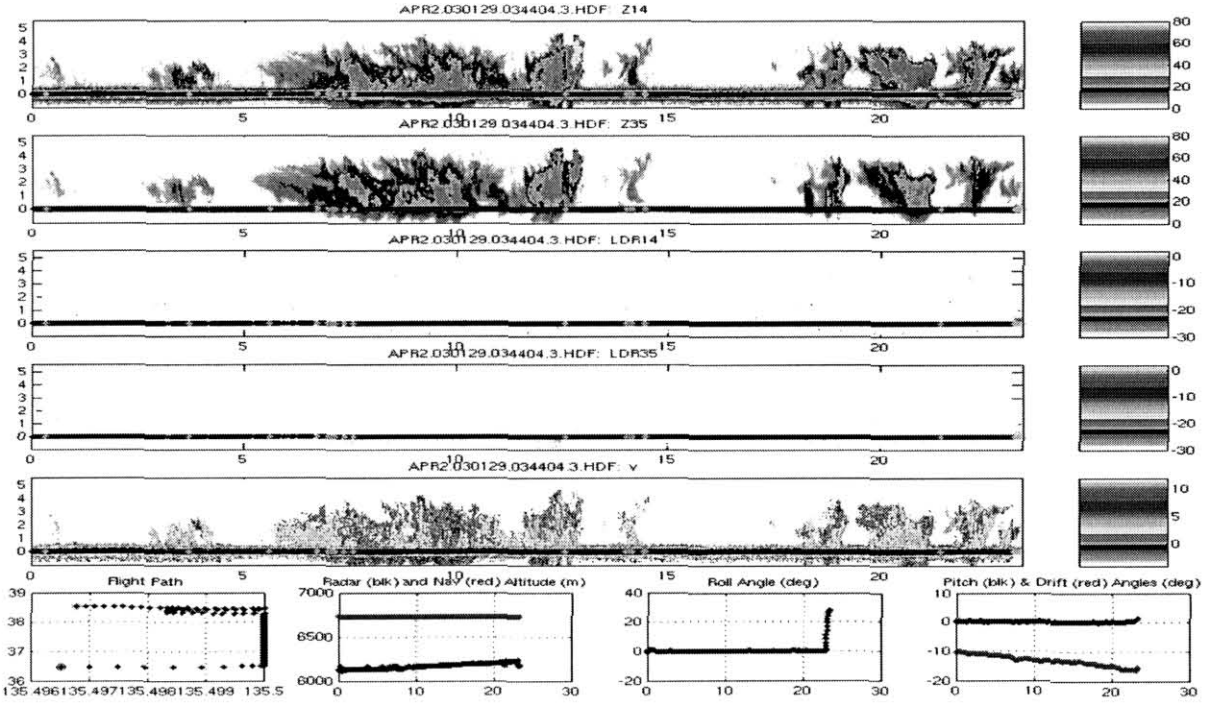

Figure 6. Snowfall over ocean. See Figure 5.